

Antiferromagnetic order is possible in ternary quasicrystal approximantsA. Ishikawa,¹ T. Fujii,² T. Takeuchi,³ T. Yamada,⁴ Y. Matsushita,⁵ and R. Tamura¹¹*Department of Materials Science and Technology, Tokyo University of Science, Niijuku, Tokyo 125-8585, Japan*²*Cryogenic Research Center, The University of Tokyo, Bunkyo, Tokyo 113-0032, Japan*³*Toyota Technological Institute, Nagoya 468-8511, Japan*⁴*Department of Applied Physics, Tokyo University of Science, Niijuku, Tokyo 125-8585, Japan*⁵*Materials Analysis Station, National Institute for Materials Science, Tsukuba, Ibaraki 305-0047, Japan* (Received 17 December 2017; revised manuscript received 28 September 2018; published 10 December 2018)

Eight years since the discovery of the binary antiferromagnetic (AFM) quasicrystal approximants Cd_6R [R. Tamura *et al.*, *Phys. Rev. B* **82**, 220201 (2010)], we report the observation of an AFM transition in quasicrystal approximants Au-Al-R ($R = \text{Gd}$ and Tb), which represent examples of AFM in *ternary* quasicrystal approximants. Magnetic susceptibility, magnetization, and specific heat coherently show that the Au-Al-R ($R = \text{Gd}$ and Tb) approximants undergo an AFM transition at $T_N = 9.4$ and 11.8 K, respectively. The AFM transitions are found near the phase boundary of the wide single-phase region where the chemical disorder is substantially low. This finding of ternary AFM approximants has far deeper implications compared with that of the binary AFM approximants: It now indicates the possibility to synthesize new AFM approximants in many other systems by the appropriate replacement of Cd with two other elements, and thus enables exploration of various magnetic orders over AFM spin icosahedra in solids, in particular, their evolution as a function of the electron-per-atom (e/a) ratio. Moreover, the finding provides us a missing route to synthesize an AFM quasicrystal by similar composition tuning.

DOI: [10.1103/PhysRevB.98.220403](https://doi.org/10.1103/PhysRevB.98.220403)

Since the discovery of icosahedral quasicrystals in 1984 [1], exploration for the electrical and magnetic properties that are *unique* to the quasicrystals, or the quasiperiodicity, has been extensively performed to date. For the magnetism, the magnetic quasicrystals, such as the first-generation Al-Mn [2–4], Al-Si-Mn [3,4], and Al-Pd-Mn [5] quasicrystals and the second-generation Zn-Mg- R ($R = \text{rare earth}$) [6,7], Cd-Mg- R , and Cd- R [8] quasicrystals, have been thoroughly investigated in the search for unprecedented quasiperiodic magnetic orders. However, all the experimental works so far have commonly shown the occurrences of a spin-glass-like behavior, if any, without any magnetic transition. On the other hand, theoretical studies of ideal quasiperiodic lattices have suggested that nontrivial magnetic orders are compatible with the quasiperiodicity [9,10]. Moreover, Lifshitz conjectured that antiferromagnetic (AFM) orders are possible for primitive and body-centered icosahedral quasicrystals, whereas they are not for face-centered icosahedral quasicrystals, based on a symmetry consideration [11].

Soon after the discovery of the binary icosahedral quasicrystal $\text{Cd}_{5.7}\text{Yb}$ in 2000 [12,13], the existence of the crystalline analogue Cd_6Yb , the so-called Tsai-type 1/1 cubic approximant, in a nearby composition was recognized [14,15], and considerable attention has been paid to its structural and physical properties in close relation to those of the quasicrystal. The Tsai-type approximants, bcc crystals (space group $Im\bar{3}$) that contain ~ 168 atoms in a unit cell, can be regarded as a bcc packing of multiple shell icosahedral clusters referred to as Tsai-type clusters: the first shell is a dodecahedron composed of 20 atoms, the second shell is an icosahedron of 12 atoms, the third shell is an icosidodecahedron of 30 atoms,

and the outermost shell is a defect rhombic triacontahedron of 60 atoms [14]. Among the multiple concentric shells, the second icosahedron shell is occupied by rare-earth (R) atoms.

A number of ternary Tsai-type 1/1 approximants have been synthesized to date, such as Ag-In- R [16–18] and Au- M - R ($M = \text{Al}$ [19–21], Ga [22,23], In [17], Si [24,25], Ge [24,26], and Sn [18,27]). The Tsai-type approximants have been a target of growing interest, not only because they have the same local atomic structure as the binary quasicrystal Cd_6Yb , but also because they exhibit a large variety of interesting phenomena, such as unique low-temperature order-disorder transitions [28–32], rich magnetic transitions [25,32–41], valence fluctuation [42,43], quantum critical phenomena [44], and superconducting transitions [45–47], none of which had been observed in quasicrystal approximants before. As far as the magnetism is concerned, no antiferromagnetism (AFM) has been reported in ternary approximants, in contrast to the AFM orders found in binary Cd_6Tb in 2010 [33]. The reason for the absence of AFM in ternary approximants has been a puzzle to date. After eight years of material exploration since the discovery of the binary AFM approximants Cd_6R , we will put an end to this unsolved issue by demonstrating here the occurrence of AFM in *ternary* approximants Au-Al-R ($R = \text{Gd}$ and Tb) after fine tuning of the composition inside the single-phase domain.

Polycrystalline alloys of the compositions $\text{Au}_{73}\text{Al}_{13}\text{Gd}_{14}$ and $\text{Au}_{72}\text{Al}_{14}\text{Tb}_{14}$ were synthesized by arc melting high-purity (>99.9 wt%) Au, Al, Gd, and Tb elements. The alloys were then annealed at 1073 K for 50 h under an Ar atmosphere, followed by quenching into chilled water to obtain a homogeneous equilibrium phase at 1073 K.

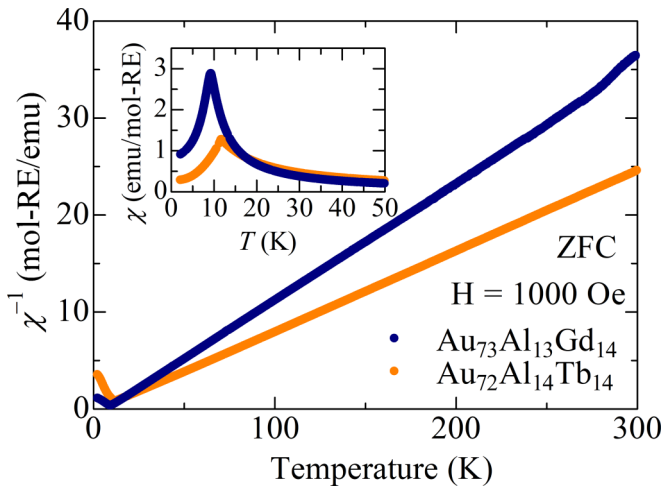


FIG. 1. Temperature dependences of the inverse magnetic susceptibility χ^{-1} , for $\text{Au}_{73}\text{Al}_{13}\text{Gd}_{14}$ and $\text{Au}_{72}\text{Al}_{14}\text{Tb}_{14}$. The inset shows the temperature dependence of the magnetic susceptibility in a low-temperature region below 50 K.

The phase purity of the samples was examined using powder x-ray diffraction (XRD; Rigaku MiniFlex600) with Cu $K\alpha$ radiation, and also scanning electron microscopy (SEM; JEOL JSM-IT100) equipped with an energy-dispersive x-ray spectroscopy (EDX) apparatus. The powder XRD patterns for $\text{Au}_{73}\text{Al}_{13}\text{Gd}_{14}$ and $\text{Au}_{72}\text{Al}_{14}\text{Tb}_{14}$ presented in the Supplemental Material [48] show that all the peaks can be indexed to a bcc crystal with lattice parameters of 14.8285 and 14.7753 Å, respectively, which indicates that a single phase is obtained for both of the nominal compositions. Data collection for crystal structure analysis was carried out for a single crystal picked from polygrain samples using a Rigaku Saturn CCD diffractometer equipped with a VariMax confocal optics for Mo $K\alpha$ radiation. Cell refinement and data reduction were carried out by using the D*TREK package in the CRYSTALCLEAR software suite [49]. Preliminary structures were solved using SHELXT [50] and refined by full-matrix least squares on F2 using the SHELXL [51] in the WinGX program package [52]. The temperature and field dependence of the magnetization were measured using a physical

property measurement system (PPMS; Quantum Design) equipped with a vibrating sample magnetometer (VSM) in the temperature range between 2.2 and 300 K and at magnetic fields up to 7 T. The temperature dependence of the magnetization was measured upon heating with a field of 10 mT after cooling to the lowest temperature with zero field (zero-field cooling; ZFC) or with a field of 10 mT (field cooling; FC). The specific heat was measured using the PPMS by the relaxation method between 1.8 and 30 K, and under fields of 0 and 9 T.

Figure 1 shows the temperature dependence of the inverse magnetic susceptibility, $1/\chi$, in the temperature range of 2.2–300 K. The susceptibilities for both systems well obey the Curie-Weiss law, $\chi = \frac{N_A \mu_{\text{eff}}^2 \mu_B^2}{3k_B(T - \Theta_p)} + \chi_0$, as manifested by the excellent linearity in the $1/\chi$ - T curves, where k_B , Θ_p , N_A , μ_{eff} , μ_B , and χ_0 are the Boltzmann constant, paramagnetic Curie temperature, Avogadro's number, effective moment, Bohr magneton, and temperature-independent magnetic susceptibility, respectively. Here, χ_0 is introduced in order to take into account the diamagnetic contribution from the sample holder and both the para- and diamagnetic contributions from the conduction electrons and the ion cores. The results of least-squares fits to the Curie-Weiss law above 50 K are $\mu_{\text{eff}} = 8.24 \mu_B$, $\Theta_p = 5.9$ K, and $\chi_0 = -6.9 \times 10^{-4}$ emu/mol-Gd for $\text{Au}_{73}\text{Al}_{13}\text{Gd}_{14}$, and $\mu_{\text{eff}} = 9.85 \mu_B$, $\Theta_p = 4.2$ K, and $\chi_0 = -3.8 \times 10^{-4}$ emu/mol-Tb for $\text{Au}_{72}\text{Al}_{14}\text{Tb}_{14}$. The values of μ_{eff} are in good agreement with the theoretical values expected for the R^{3+} free ions, $7.94 \mu_B$ and $9.72 \mu_B$, respectively, which indicates that the R^{3+} spins are well localized on the vertices of the icosahedron for both compounds. The paramagnetic Curie temperature Θ_p can be regarded as the net interspin interaction; therefore, positive Θ_p values indicate that the net interaction on each spin is ferromagnetic for both the Au-Al-Gd and Au-Al-Tb approximants.

Figures 2(a) and 2(b) show the temperature dependence of the ZFC and FC magnetic susceptibilities for $\text{Au}_{73}\text{Al}_{13}\text{Gd}_{14}$ and $\text{Au}_{72}\text{Al}_{14}\text{Tb}_{14}$, respectively. The occurrences of magnetic transitions are clearly evidenced by sharp cusps at $T_N = 9.4$ K and $T_N = 11.8$ K for $\text{Au}_{73}\text{Al}_{13}\text{Gd}_{14}$ and $\text{Au}_{72}\text{Al}_{14}\text{Tb}_{14}$, respectively. In addition, no appreciable difference is noticed between the ZFC and FC curves for both systems, showing the absence of spin-freezing behavior in the present compounds.

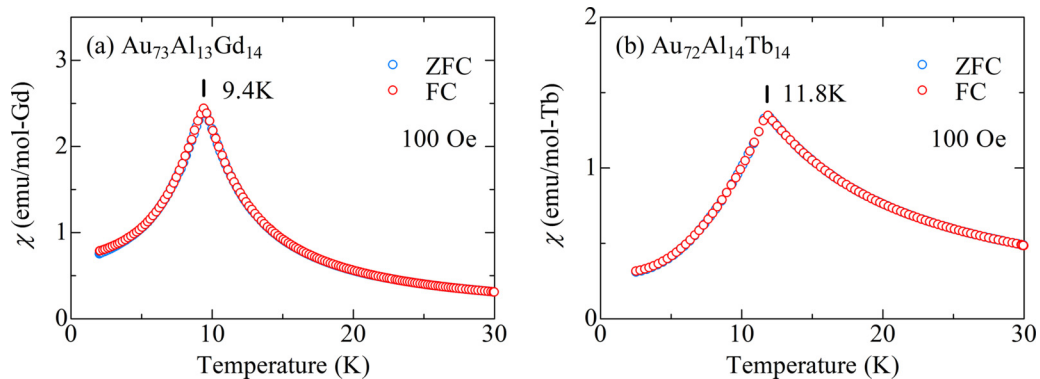


FIG. 2. Temperature dependences of ZFC and FC magnetic susceptibilities for (a) $\text{Au}_{73}\text{Al}_{13}\text{Gd}_{14}$ and (b) $\text{Au}_{72}\text{Al}_{14}\text{Tb}_{14}$ in a low-temperature region below 30 K. A sharp cusp is observed at $T_N = 9.4$ and 11.8 K, respectively, showing an occurrence of an AFM transition at T_N .

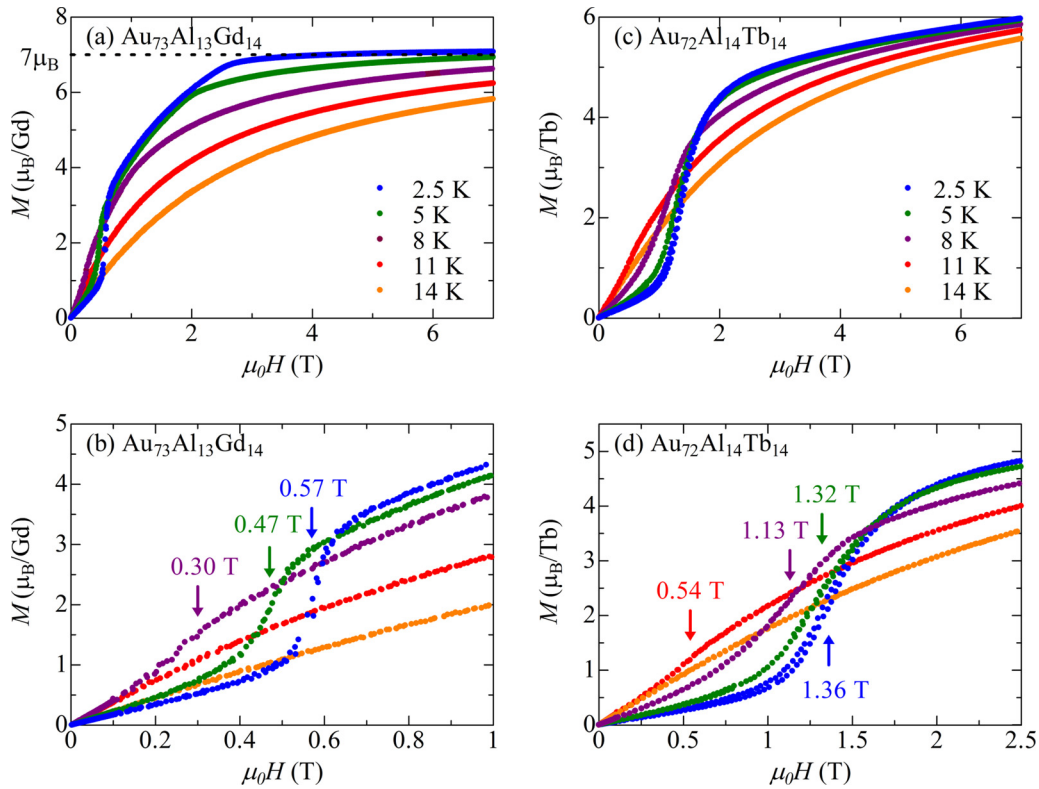


FIG. 3. The magnetization M for (a) $\text{Au}_{73}\text{Al}_{13}\text{Gd}_{14}$ and (c) $\text{Au}_{72}\text{Al}_{14}\text{Tb}_{14}$ as a function of magnetic field up to 7 T. (b) and (c) show enlarged magnetization curves at lower fields, respectively. For $\text{Au}_{73}\text{Al}_{13}\text{Gd}_{14}$, magnetic saturation to $7\mu_{\text{B}}/\text{Gd}$ occurs below 3 T at 2.5 K. A spin flop is noticed at the fields indicated by arrows. H_{SF} increases with decreasing temperature, confirming an occurrence of an AFM transition for both of the compounds.

Figures 3(a) and 3(c) show the magnetic field dependence of the magnetization M for $\text{Au}_{73}\text{Al}_{13}\text{Gd}_{14}$ and $\text{Au}_{72}\text{Al}_{14}\text{Tb}_{14}$, respectively, in fields up to 7 T, while Figs. 3(b) and 3(d) show enlarged magnetization curves at lower fields, respectively. Below T_{N} , a single metamagnetic anomaly is clearly observed for both the Au-Al-Gd and Au-Al-Tb approximants with the occurrence of a spin flop at low fields. The magnetic field corresponding to the spin flop, H_{SF} , increases with a decrease in temperature. Both the metamagnetic anomaly and the shift of H_{SF} toward higher fields with decreasing temperature

clearly indicate that the transitions are antiferromagnetic. For $\text{Au}_{73}\text{Al}_{13}\text{Gd}_{14}$, the magnetization reaches the full moment of $7\mu_{\text{B}}/\text{Gd}^{3+}$ under a field of 3 T at 2.5 K, whereas for $\text{Au}_{72}\text{Al}_{14}\text{Tb}_{14}$, the magnetization gradually increases with the magnetic field above H_{SF} and reaches $\sim 6\mu_{\text{B}}/\text{Tb}^{3+}$ at 7 T, which is $2/3$ of the full moment ($9\mu_{\text{B}}/\text{Tb}^{3+}$) expected from a free Tb^{3+} ion. Such unsaturated behavior of $\text{Au}_{72}\text{Al}_{14}\text{Tb}_{14}$ is attributed to the magnetic anisotropy of Tb^{3+} spins, which is absent for isotropic Gd^{3+} spins. The magnetic anisotropies of Tb^{3+} spins have also been recognized in other Tsai-type

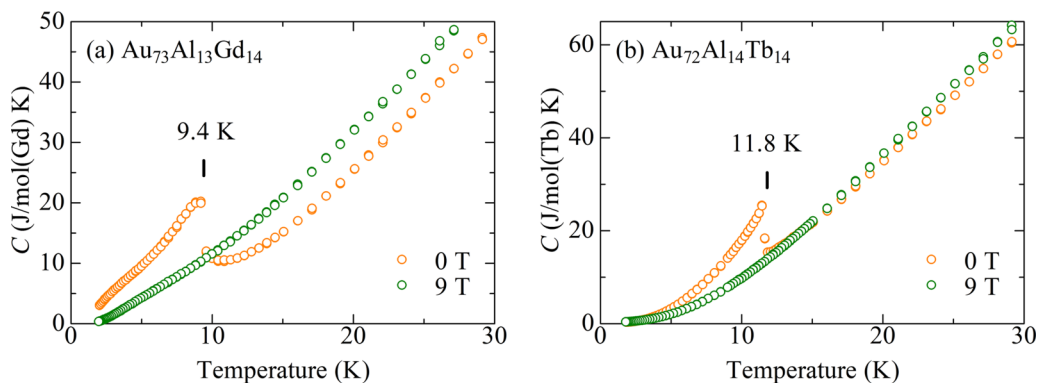


FIG. 4. Temperature dependences of the specific heat measured at zero and 9 T for (a) $\text{Au}_{73}\text{Al}_{13}\text{Gd}_{14}$ and (b) $\text{Au}_{72}\text{Al}_{14}\text{Tb}_{14}$. A lambda anomaly due to the AFM transition is clearly observed for both of the compounds. The anomaly is suppressed under the field of 9 T, which is consistent with the occurrence of the antiferromagnetic transitions.

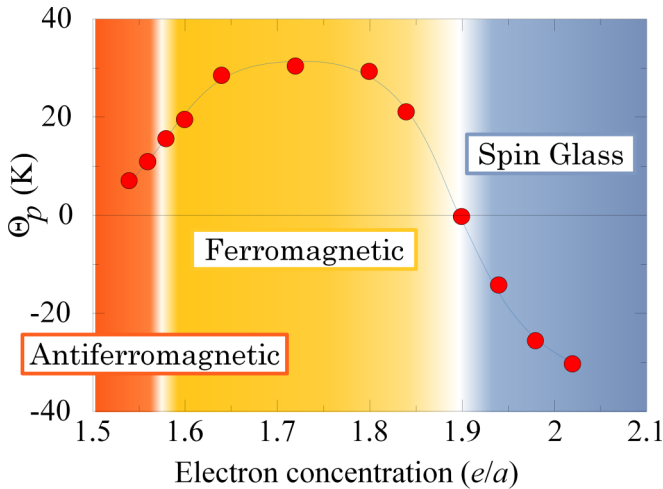


FIG. 5. The paramagnetic Curie temperature Θ_p vs the average electron-per-atom (e/a) ratio for the Au-Al-Gd approximant, together with the magnetic orders observed at 2.2 K. The AFM order is found near the phase boundary within a narrow electron concentration window of $e/a \sim 1.54$ – 1.56 , where Θ_p is weakly positive.

approximants [25,39]. The existence of a uniaxial magnetic anisotropy along a pseudofivefold axis of the Tb icosahedron is suggested from an inelastic neutron-scattering experiment performed for the Au-Si-Tb approximant [53]. Figures 4(a) and 4(b) show the temperature dependence of the specific heat for $\text{Au}_{73}\text{Al}_{13}\text{Gd}_{14}$ and $\text{Au}_{72}\text{Al}_{14}\text{Tb}_{14}$, respectively, measured at zero field and 9 T. A well-defined lambda anomaly, characteristic to second-order transitions, is observed at T_N for both the compounds at zero field, which is consistent with the occurrence of the AFM transition at T_N . These anomalies disappear under a magnetic field of 9 T for both compounds, as shown in Figs. 4(a) and 4(b), which indicates the suppression of the AFM order at higher fields above H_{SF} .

Figure 5 shows the condition for the occurrence of the AFM order in the Au-Al-Gd approximant in terms of the average electron-per-atom (e/a) ratio, where we assume that Au is monovalent and both Al and Gd are trivalent. Ferromagnetic orders and spin-glass behaviors are observed in a relatively wide e/a regions [41]. By contrast, the AFM order is found to exist within a narrow e/a window of $e/a \sim 1.54$ – 1.56 , at compositions near the phase boundary of the wide single-phase region. The fact that Θ_p depends on e/a is understood on the basis of the Ruderman-Kittel-Kasuya-Yoshida (RKKY) interaction. The RKKY interaction between a pair of spins oscillate as a function of $k_F R$, where R is the distance between the two spins. The substitution of Au for Al changes both k_F and R . However, their product $k_F R$ is solely dependent on the e/a ratio on the basis of the free-electron approximation when the fractional coordinates of the R positions do not vary with the lattice parameter. This is indeed really the case for Tsai-type 1/1 approximants: the fractional coordinates of the R atoms are the same within $\sim 1\%$ difference for all the Tsai-type 1/1 approximants reported. Since Θ_p can be regarded as the sum of the interactions over all spin pairs, it follows that Θ_p is also solely dependent on e/a . Concerning the values of Θ_p for the ternary AFM approximants, the weakly positive Θ_p clearly indicates that both ferromagnetic and antiferromagnetic interactions coexist and, in addition, the former is stronger than the latter for both $\text{Au}_{73}\text{Al}_{13}\text{Gd}_{14}$ and $\text{Au}_{72}\text{Al}_{14}\text{Tb}_{14}$, which is in contrast to the cases of the binary AFM Cd_6R approximants where Θ_p are negative.

Figure 6 shows the results of the structural refinements on $\text{Au}_{73}\text{Al}_{13}\text{Gd}_{14}$ and $\text{Au}_{72}\text{Al}_{14}\text{Tb}_{14}$. The refined structural parameters are listed in Table I and more information on the structures is given in the Supplemental Material [48]. For both compounds, the center of the Tsai-type cluster is occupied by four nonmagnetic Au/Al atoms, which forms a tetrahedron, and the icosahedron shell is exclusively occupied by R atoms. Thus, the magnetic moments are found to be

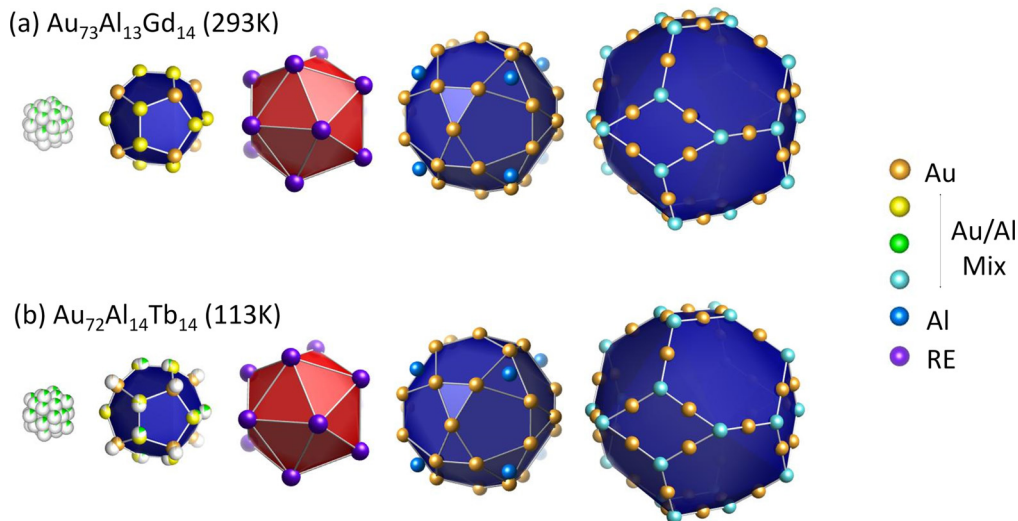


FIG. 6. The Tsai-type icosahedral cluster of (a) $\text{Au}_{73}\text{Al}_{13}\text{Gd}_{14}$ and (b) $\text{Au}_{72}\text{Al}_{14}\text{Tb}_{14}$ obtained from the single-crystal structural refinements. The centers of both clusters are occupied by four nonmagnetic Au/Al atoms that form a tetrahedron with disordered orientation. Magnetic atoms are found solely on the vertices of the second icosahedron shell, justifying that both compounds can be regarded as a bcc packing of spin icosahedra.

TABLE I. Refined structural parameters of $\text{Au}_{73}\text{Al}_{13}\text{Gd}_{14}$ and $\text{Au}_{72}\text{Al}_{14}\text{Tb}_{14}$.

Au ₇₃ Al ₁₃ Gd ₁₄ [Im $\bar{3}$, $a = 14.8072(8)$ Å, $R1 = 2.91\%$]						
Site	Wyckoff position	Occ.	x	y	z	$U_{\text{eq}}(\text{Å}^2)$
Au1	48 <i>h</i>	1	0.15447(3)	0.60826(3)	0.70082(3)	0.01777(12)
Au2/Al2	24 <i>g</i>	0.940(4)/0.060(4)	0.26133(5)	0.5	0.59049(4)	0.0224(2)
Au3	24 <i>g</i>	1	0	0.34892(4)	0.59468(4)	0.01724(14)
Au4	16 <i>f</i>	1	0.34713(3)	0.65287(3)	0.65287(3)	0.02477(18)
Au5/Al5	12 <i>e</i>	0.184(5)/0.816(5)	0	0.5	0.68888(19)	0.0161(9)
Au6	12 <i>d</i>	1	0.09295(6)	0.5	0.5	0.0264(2)
Al8	8 <i>c</i>	1	0.25	0.75	0.75	0.0236(17)
Au7A/Al7A	16 <i>f</i>	0.0914(8)/0.0801(7)	0.4450(3)	0.4450(3)	0.5550(3)	0.048(3)
Au7B/Al7B	24 <i>g</i>	0.0784(6)/0.0687(5)	0.4122(7)	0.5	0.4576(10)	0.053(3)
Au7C/Al7C	24 <i>g</i>	0.0383(6)/0.0335(5)	0.4380(15)	0.5	0.5955(16)	0.043(5)
Gd1	24 <i>g</i>	1	0.19739(5)	0.68493(5)	0.5	0.01430(15)
Au ₇₂ Al ₁₄ Tb ₁₄ [Im $\bar{3}$, $a = 14.7844(16)$ Å, $R1 = 4.20\%$]						
Site	Wyckoff position	Occ.	x	y	z	$U_{\text{eq}}(\text{Å}^2)$
Au1	48 <i>h</i>	1	0.10784(2)	0.34519(2)	0.20098(2)	0.01360(7)
Au2A/Al2A	24 <i>g</i>	0.867(4)/0.094(4)	0.26200(5)	0.40937(4)	0.5	0.01720(15)
Au2B/Al2B	24 <i>g</i>	0.03570(16)/0.00387(16)	0	0.2433(13)	0.0667(12)	0.01720(15)
Au3	24 <i>g</i>	1	0.09485(3)	0.15032(3)	0.5	0.01277(8)
Au4A	16 <i>f</i>	0.974(5)	0.34753(6)	0.34753(6)	0.34753(6)	0.0210(2)
Au4B	16 <i>f</i>	0.026(5)	0.328(2)	0.328(2)	0.328(2)	0.0210(2)
Au5/Al5	12 <i>e</i>	0.123(5)/0.877(5)	0	0.3108(2)	0.5	0.0116(8)
Au6	12 <i>d</i>	1	0.09340(5)	0.5	0.5	0.01888(13)
Al8	8 <i>c</i>	1	0.25	0.25	0.25	0.0179(13)
Au7A/Al7A	16 <i>f</i>	0.0922(10)/0.0469(5)	0.4441(3)	0.4441(3)	0.4441(3)	0.0327(19)
Au7B/Al7B	24 <i>g</i>	0.0813(7)/0.0413(3)	0.4116(5)	0.4586(6)	0.5	0.0258(14)
Au7C/Al7C	24 <i>g</i>	0.0782(7)/0.0397(3)	0.401(3)	0.5	0.433(2)	0.137(13)
Tb1	24 <i>g</i>	1	0.31503(4)	0.19707(4)	0.5	0.01189(9)

located solely at the vertices of the icosahedron as in the cases of Cd_6R . In addition, the so-called cubic interstices (Al8), which are sometimes subject to partial occupation in the cases of Cd_6R , are found to be fully occupied exclusively by Al atoms in both compounds. One significant feature of the present compounds is that the Au/Al mix sites are almost fully occupied by Au atoms as a consequence of the high Au concentrations. Both of the above features point to low positional and chemical disorders in the present ternary compounds. Considering that AFM orders have only been observed in binary Cd_6R having no chemical disorder, the suppression of the disorders may be partly responsible for the occurrence of the AFM orders in the present ternary approximants. Further work is certainly needed to clarify this point.

The observation of the metamagnetic anomaly in the Au-Al-Gd approximant is of particular interest since a Gd^{3+} spin is isotropic owing to the S nature ($L = 0$) of the $4f$ electron cloud. In this respect, theoretical studies by Schröder *et al.* [54], have shown the existence of a metamagnetic anomaly in an antiferromagnetic Heisenberg icosahedron without magnetic anisotropy. The metamagnetic anomaly is a direct consequence of the magnetic frustration over the antiferromagnetic icosahedron. Thus, their result provides one possible explanation for our observation of the metamagnetic anomaly in the Au-Al-Gd approximant.

In conclusion, we have reported AFM transitions in *ternary* quasicrystal approximants after fine composition tuning. Both the magnetic susceptibility and the specific heat coherently indicate that $\text{Au}_{73}\text{Al}_{13}\text{Gd}_{14}$ and $\text{Au}_{72}\text{Al}_{14}\text{Tb}_{14}$ undergo AFM transitions at $T_N = 9.4$ and 11.8 K, respectively. A single metamagnetic anomaly is observed at $H_{\text{SF}} = 0.57$ and 1.36 T, respectively, at 2.5 K, showing an occurrence of a spin flop at H_{SF} . The AFM orders in the ternary Au-Al-R approximants are observed at compositions near the phase boundary of the wide single-phase region, where chemical disorder is substantially low, which might be partly responsible for the occurrence of the AFM transition in both of the compounds. This finding of the ternary AFM approximants has far deeper implications than that of the binary AFM approximants because it now provides us with a procedure to obtain a number of new AFM approximants in a variety of ternary systems by the replacement of Cd with two other elements followed by fine composition tuning, and thus enables more detailed exploration of the various magnetic orders over AFM spin icosahedra in various spin systems. Moreover, we are also provided with a missing route to realize an AFM quasicrystal by similar composition tuning, a work which is presently in progress.

This work was supported by Kakenhi Grant-in-Aid No. 16H04018 from the Japan Society for the Promotion of Science (JSPS).

- [1] D. Shechtman, I. Blech, D. Gratias, and J. W. Cahn, *Phys. Rev. Lett.* **53**, 1951 (1984).
- [2] K. Fukamichi, T. Masumoto, M. Oguchi, A. Inoue, T. Goto, T. Sakakibara, and S. Todo, *J. Phys. F: Met. Phys.* **16**, 1059 (1986).
- [3] W. W. Warren, H.-S. Chen, and G. P. Espinosa, *Phys. Rev. B* **34**, 4902(R) (1986).
- [4] J. J. Hauser, H. S. Chen, and J. V. Waszczak, *Phys. Rev. B* **33**, 3577 (1986).
- [5] F. Hippert and J. J. Prejean, *Philos. Mag.* **88**, 2175 (2008).
- [6] Y. Hattori, A. Niikura, A. P. Tsai, A. Inoue, T. Masumoto, K. Fukamichi, H. Aruga-Katori, and T. Goto, *J. Phys.: Condens. Matter* **7**, 2313 (1995).
- [7] T. J. Sato, H. Takakura, A. P. Tsai, and K. Shibata, *Phys. Rev. Lett.* **81**, 2364 (1998).
- [8] T. J. Sato, J. Guo, and A. P. Tsai, *J. Phys.: Condens. Mater.* **13**, L105 (2001).
- [9] Y. Achiam, T. C. Lubensky, and E. W. Marshall, *Phys. Rev. B* **33**, 6460 (1986).
- [10] H. Tsunetsugu, T. Fujiwara, K. Ueda, and T. Tokihiro, *J. Phys. Soc. Jpn.* **55**, 1420 (1986).
- [11] R. Lifshitz, *Phys. Rev. Lett.* **80**, 2717 (1998).
- [12] A. P. Tsai, J. Q. Guo, E. Abe, H. Takakura, and T. J. Sato, *Nature (London)* **408**, 537 (2000).
- [13] J. Q. Guo, E. Abe, and A. P. Tsai, *Phys. Rev. B* **62**, R14605 (2000).
- [14] C. P. Gómez and S. Lidin, *Phys. Rev. B* **68**, 024203 (2003).
- [15] A. P. Tsai, *Chem. Soc. Rev.* **42**, 5352 (2013).
- [16] L. V. Sysa, Ya. M. Kalychak, Ya. V. Galadzhun, V. I. Zaremba, L. G. Akselrud, and R. V. Skolozdra, *J. Alloys Compd.* **266**, 17 (1998).
- [17] J. F. Ruan, K. H. Kuo, J. Q. Guo, and A. P. Tsai, *J. Alloys Compd.* **370**, L23 (2004).
- [18] Y. Morita and A. P. Tsai, *Jpn. J. Appl. Phys.* **47**, 7975 (2008).
- [19] T. Ishimasa, Y. Tanaka, and S. Kashimoto, *Philos. Mag.* **91**, 4218 (2011).
- [20] K. Tanaka, Y. Tanaka, T. Ishimasa, M. Nakayama, S. Matsukawa, K. Deguchi, and N. K. Sato, *Acta Phys. Pol. A* **126**, 603 (2014).
- [21] Y.-G. So, K. Kimoto, and K. Edagawa, *Mater. Trans.* **56**, 495 (2015).
- [22] S. Matsukawa, K. Tanaka, M. Nakayama, K. Deguchi, K. Imura, H. Takakura, S. Kashimoto, T. Ishimasa, and N. K. Sato, *J. Phys. Soc. Jpn.* **83**, 034705 (2014).
- [23] Y. Verbovytskyy, *Chem. Met. Alloys* **7**, 42 (2014).
- [24] G. H. Gebresenbut, R. Tamura, D. Eklöf, and C. P. Gómez, *J. Phys.: Condens. Matter* **25**, 135402 (2013).
- [25] G. H. Gebresenbut, M. S. Andersson, P. Nordblad, M. Sahlberg, and C. P. Gómez, *Inorg. Chem.* **55**, 2001 (2016).
- [26] Q. Lin and J. D. Corbett, *Inorg. Chem.* **49**, 4570 (2010).
- [27] P. Boulet, D. Mazzone, H. Noël, P. Rogl, and R. Ferro, *J. Alloys Compd.* **317**, 350 (2001).
- [28] R. Tamura, Y. Murao, S. Takeuchi, M. Ichihara, M. Isobe, and Y. Ueda, *Jpn. J. Appl. Phys.* **41**, L524 (2002).
- [29] T. Ishimasa, Y. Kasano, A. Tachibana, S. Kashimoto, and K. Osaka, *Philos. Mag.* **87**, 2887 (2007).
- [30] T. Yamada, R. Tamura, Y. Muro, K. Motoya, M. Isobe, and Y. Ueda, *Phys. Rev. B* **82**, 134121 (2010).
- [31] K. Nishimoto, T. Sato, and R. Tamura, *J. Phys.: Condens. Mater.* **25**, 235403 (2013).
- [32] R. Tamura, *J. Phys.: Condens. Mater.* **27**, 085401 (2015).
- [33] R. Tamura, Y. Muro, T. Hiroto, K. Nishimoto, and T. Takabatake, *Phys. Rev. B* **82**, 220201(R) (2010).
- [34] M. G. Kim, G. Beutier, A. Kreyssig, T. Hiroto, T. Yamada, J. W. Kim, M. de Boissieu, R. Tamura, and A. I. Goldman, *Phys. Rev. B* **85**, 134442 (2012).
- [35] R. Tamura, Y. Muro, T. Hiroto, H. Yaguchi, G. Beutier, and T. Takabatake, *Phys. Rev. B* **85**, 014203 (2012).
- [36] A. Mori, H. Ota, S. Yoshiuchi, K. Iwakawa, Y. Taga, Y. Hirose, T. Takeuchi, E. Yamamoto, Y. Haga, F. Honda, R. Settai, and Y. Onuki, *J. Phys. Soc. Jpn.* **81**, 024720 (2012).
- [37] A. Kreyssig, G. Beutier, T. Hiroto, M. G. Kim, G. S. Tucker, M. de Boissieu, R. Tamura, and A. I. Goldman, *Philos. Mag. Lett.* **93**, 512 (2013).
- [38] T. Hiroto, G. H. Gebresenbut, C. P. Gómez, Y. Muro, M. Isobe, Y. Ueda, K. Tokiwa, and R. Tamura, *J. Phys.: Condens. Mater.* **25**, 426004 (2013).
- [39] T. Hiroto, K. Tokiwa, and R. Tamura, *J. Phys.: Condens. Mater.* **26**, 216004 (2014).
- [40] G. H. Gebresenbut, M. S. Andersson, P. Beran, P. Manuel, P. Nordblad, M. Sahlberg, and C. P. Gómez, *J. Phys.: Condens. Mater.* **26**, 322202 (2014).
- [41] A. Ishikawa, T. Hiroto, K. Tokiwa, T. Fujii, and R. Tamura, *Phys. Rev. B* **93**, 024416 (2016).
- [42] D. Kawana, T. Watanuki, A. Machida, T. Shobu, K. Aoki, and A. P. Tsai, *Phys. Rev. B* **81**, 220202(R) (2010).
- [43] T. Watanuki, S. Kashimoto, D. Kawana, T. Yamazaki, A. Machida, Y. Tanaka, and T. J. Sato, *Phys. Rev. B* **86**, 094201 (2012).
- [44] K. Deguchi, S. Matsukawa, N. K. Sato, T. Hattori, K. Ishida, H. Takakura, and T. Ishimasa, *Nat. Mater.* **11**, 1013 (2012).
- [45] K. Deguchi, M. Nakayama, S. Matsukawa, K. Imura, K. Tanaka, T. Ishimasa, and N. K. Sato, *J. Phys. Soc. Jpn.* **84**, 023705 (2015).
- [46] K. Deguchi, M. Nakayama, S. Matsukawa, K. Imura, K. Tanaka, T. Ishimasa, and N. K. Sato, *J. Phys. Soc. Jpn.* **84**, 015002 (2015).
- [47] K. Kamiya, T. Takeuchi, N. Kabeya, N. Wada, T. Ishimasa, A. Ochiai, K. Deguchi, K. Imura, and N. K. Sato, *Nat. Commun.* **9**, 154 (2018).
- [48] See Supplemental Material at <http://link.aps.org/supplemental/10.1103/PhysRevB.98.220403> for the powder x-ray diffraction patterns for the Au₇₃Al₁₃Gd₁₄ and Au₇₂Al₁₄Tb₁₄ compounds. In addition, we have listed the detailed structural information on both compounds obtained from the structural refinements.
- [49] Rigaku Corporation, computer code CRYSTALCLEAR, Tokyo, Japan (2005).
- [50] G. M. Sheldrick, *Acta Cryst.* **A71**, 3 (2015).
- [51] G. M. Sheldrick, *Acta Cryst.* **C71**, 3 (2015).
- [52] L. J. Farrugia, *J. Appl. Cryst.* **32**, 837 (1999).
- [53] P. Das, P.-F. Lory, R. Flint, T. Kong, T. Hiroto, S. L. Bud'Ko, P. C. Canfield, M. de Boissieu, A. Kreyssig, and A. I. Goldman, *Phys. Rev. B* **95**, 054408 (2017).
- [54] C. Schröder, H. J. Schmidt, J. Schnack, and M. Luban, *Phys. Rev. Lett.* **94**, 207203 (2005).